Supplemental Data

Supplemental Figure S1. Phylogenetic tree of starch synthases (SSs) and glycogen synthases (GSs).

Supplemental Figure S2. Sites of *Tos17* insertion in the *OsSSIVb* gene and identification of the *Tos17* rice mutant lines by PCR.

Supplemental Figure S3. Morphological characterization of seeds from single and double mutants.

Supplemental Figure S4. Comparison of the total amounts of major lipids in bran and polished rice grain in *ss3a ss4b* and the wild-type.

Supplemental Figure S5. Immuno-electron microscopy showing the distributions of SS isozymes.

Supplemental Figure S6. Starch traits in allelic mutant lines of *ss4b* and *ss3a ss4b*.

Supplemental Figure S7. Amylopectin chain-length distribution pattern in developing endosperm of mutant lines.

Supplemental Figure S8. X-ray diffraction patterns of endosperm starch in wild-type Nipponbare and mutant lines.

Supplemental Figure S9. Native PAGE gel stained for starch biosynthesis enzyme activity in developing endosperm of wild-type Nipponbare and mutant lines.

Supplemental Figure S10. Immunoblotting analyses with antibodies against SSIVb, SSIVa, FtsZ1, FtsZ2-1, MinD, MinE, and ISA3.

Supplemental Figure S11. Pleiotropic effects of SSIIIa and SSIVb deficiency on GBSSI protein levels and AGPase activity.

Supplemental Figure S12. Recombinant SSIVb (rSSIVb) exhibits starch synthase activity.

Supplemental Figure S13. Possible model of amyloplast development in early endosperm cells of wild-type and *ss3a ss4b*.

Supplemental Figures

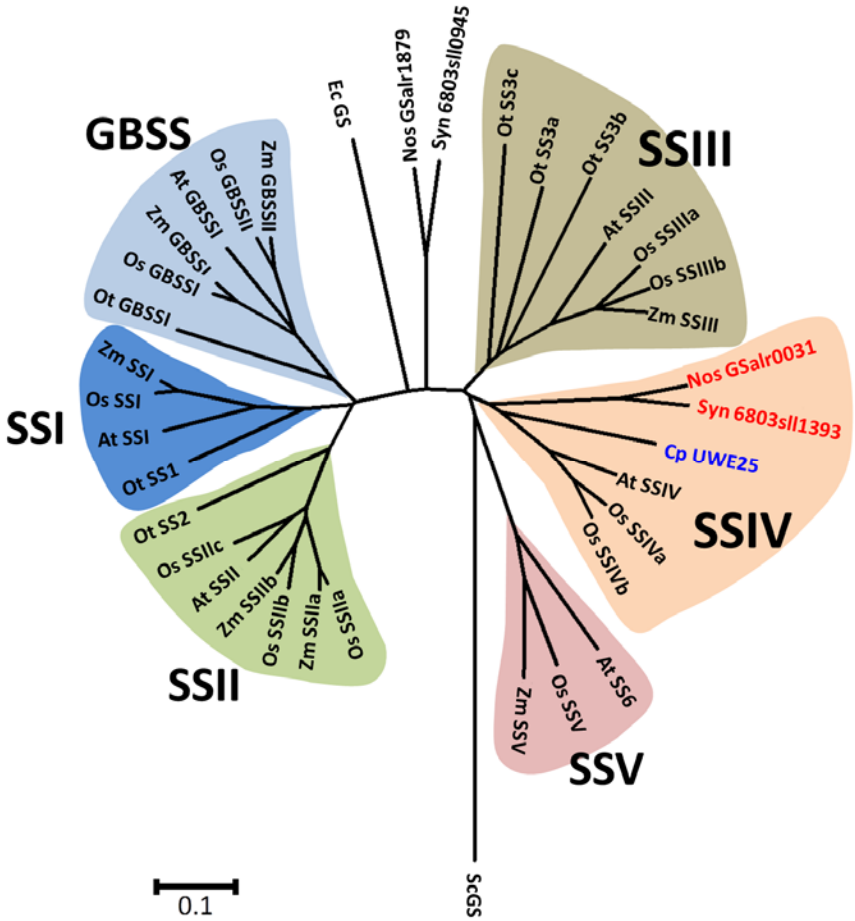

Supplemental Figure S1. Phylogenetic tree of starch synthases (SSs) and glycogen synthases (GSs). The dendrogram was generated by the neighbor-joining method using MEGA software and shows the phylogenetic relationships between the GS and SS genes. Scale bar, 0.1 amino acid substitutions per site. Sequence alignments are shown in Supplemental Table S5.

GS from *Saccharomyces cerevisiae* (Sc GS) was used as an outgroup. At, *Arabidopsis thaliana*; Cp, *Candidatus protochlamydia amoebophyla*; Ec, *Escherichia coli*; *Nos*, *Nostoc* sp. PCC 7120; Os, *Oryza sativa* (rice); Ot, *Ostreococcus tauri*; Syn, *Synechococcus* sp. PCC 6803; Vu, *Vigna unguiculata* (cow pea); Zm, *Zea mays* (maize).

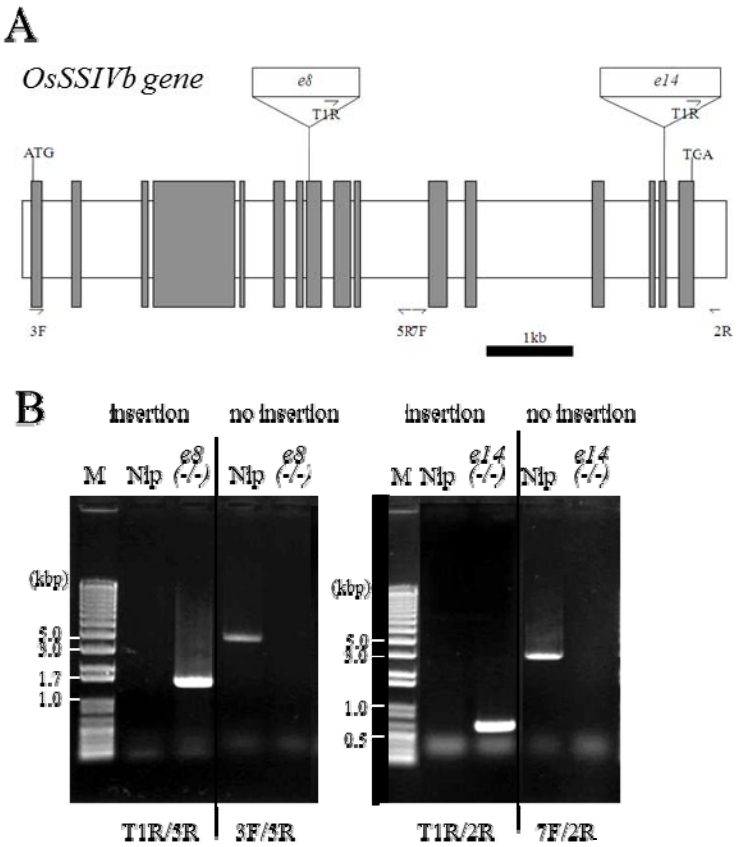

Supplemental Figure S2. Sites of *Tos17* insertion in the *OsSSIVb* gene and identification of the *Tos17* rice mutant lines by PCR. A. Structure of the *OsSSIVb* gene, which is composed of 16 exons (gray boxes) and 15 introns (white boxes). ATG, translation initiation codon; TAG, stop codon. The *Tos17* insertion sites in mutant lines (*e8* and *e14*) are indicated. Horizontal half-arrows show the locations of the PCR primers used for genotype determination and mutant line screening. Primer T1R was designed from the *Tos17* sequence, and primers 3F, 7F, 2R, and 5R were designed from the *OsSSIVb* sequence. B. Genotype determination by PCR. Primer pairs are indicated below the agarose gels. M, molecular markers; Nip, wild-type Nipponbare; *e8* (−/−), a line homozygous for *Tos17* insertion in exon 8; *e14* (−/−), a line homozygous for *Tos17* insertion in exon 14.

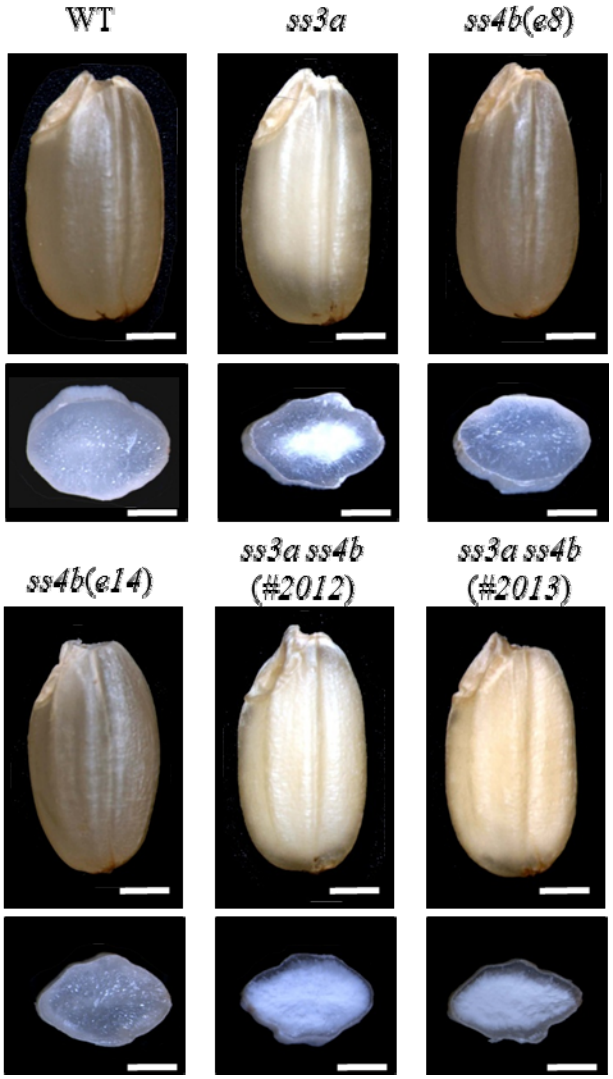

Supplemental Figure S3. Morphological characterization of seeds from single and double mutants. Upper panels, whole seed morphology. Lower panels, seed cross-sections. WT, wild-type Nipponbare. Bars = 1 mm.

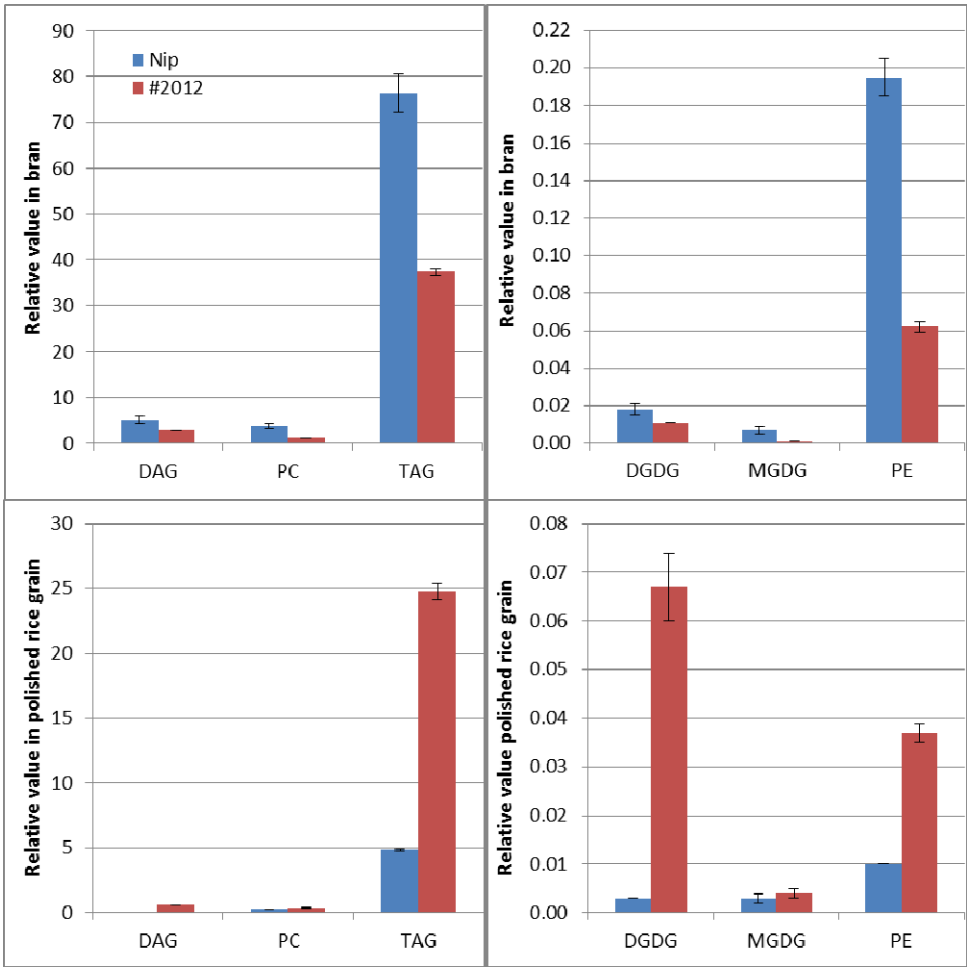

Supplemental Figure S4. Comparison of the total amounts of DAG, PC, TAG, DGDG, MGDG, and PE in bran and polished rice grains in *ss3a ss4b* (#2012) and the wild-type (Nip). Relative values were calculated based on the internal standard (PC 20:0). DAG, diacyl glycerol; PC, phosphatidylcholine; TAG, triacylglycerol; DGDG, digalactosyldiacylglycerol; MGDG, monogalactosyldiacylglycerol; PE, phosphatidylethanolamine.

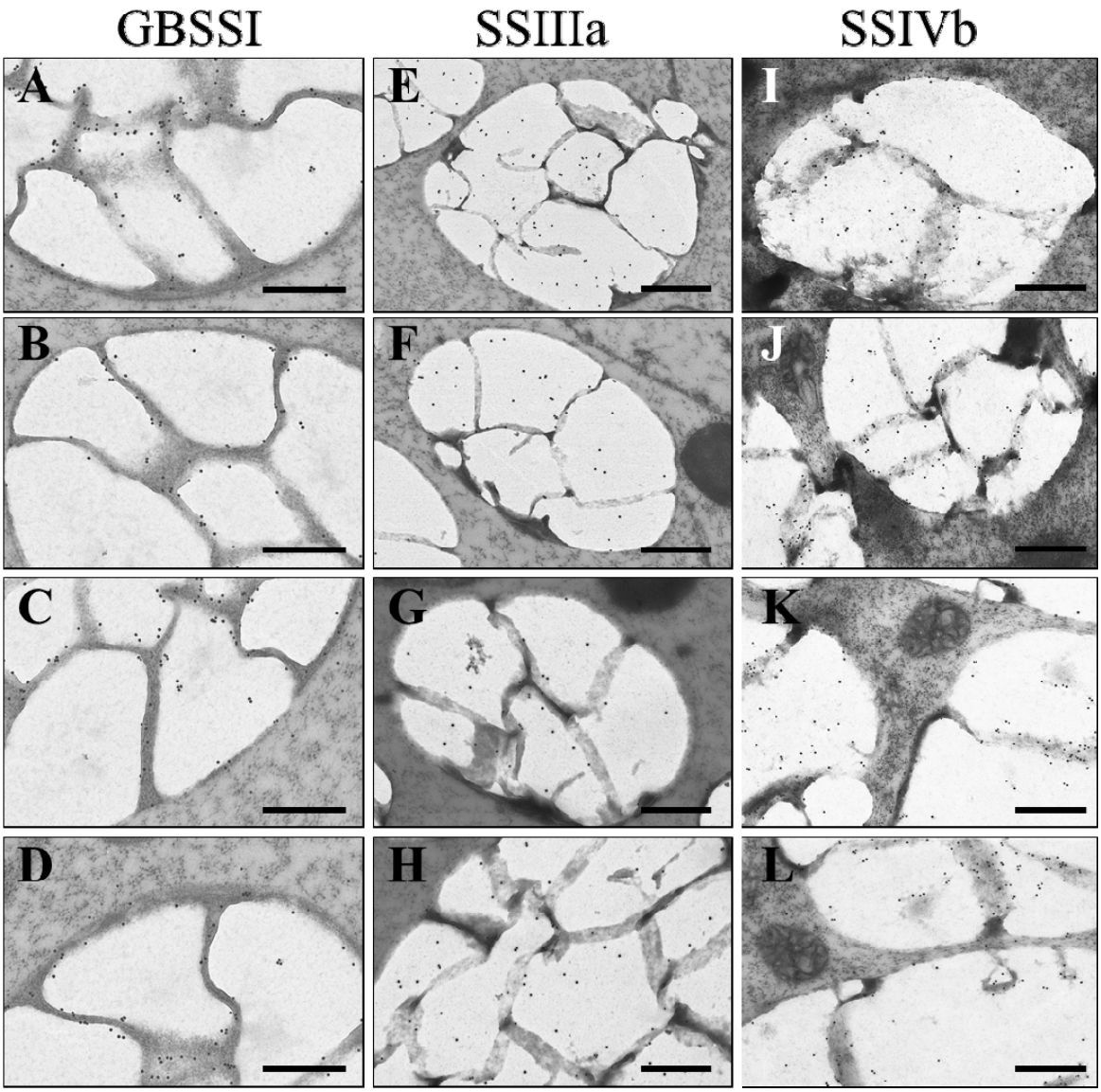

Supplemental Figure S5. Immuno-electron microscopy showing the distributions of SS isozymes.

Localization of GBSSI (A-D), SSIIIa (E-H) and SSIVb (I-L) in developing wild type endosperm are indicated by gold particles. Bars = 500 nm.

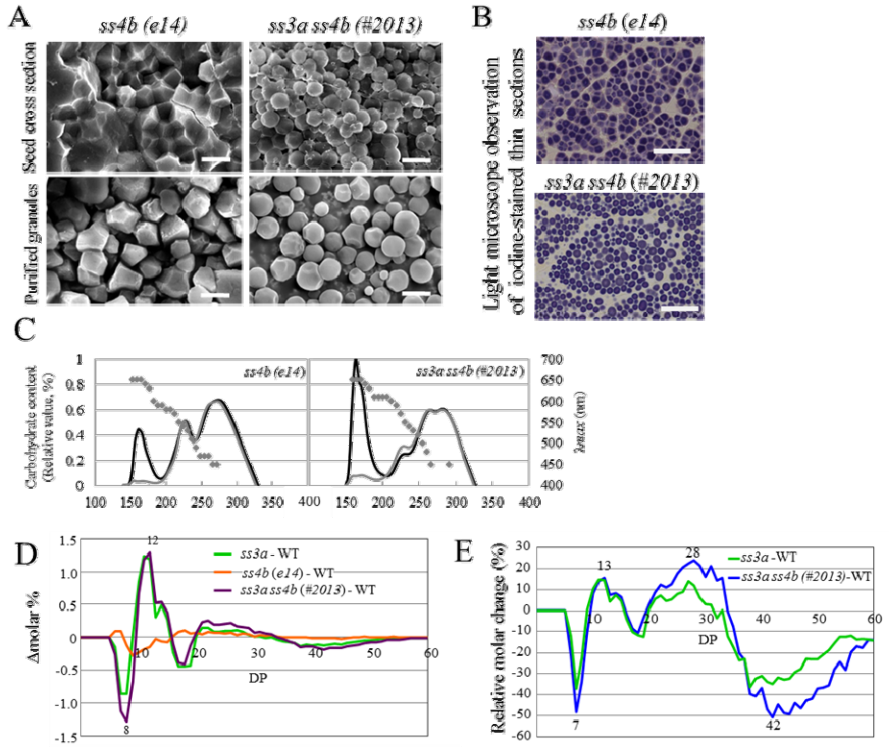

Supplemental Figure S6. Starch traits in allelic mutant lines of *ss4b* and *ss3a ss4b*. A. Scanning electron micrographs (SEM) of cross-sections of mature seeds (upper panels) and purified starch granules (lower panels). Bars = 5 μm. B. Light microscope observations of thin iodine-stained cross-sections of mature seeds. Bars = 20 μm. C. Elution profiles of isoamylase-debranched starch (black line) and amylopectin (gray line) purified by gel filtration chromatography through Toyopearl HW55S-HW50S columns. D. Comparison of differences in chain-length distribution patterns (Δ molar %) among wild-type (WT, Nipponbare), *ss3a*, *ss4b* (*e14*), and *ss3a ss4b* (*#2013*). E. Relative molar changes of each chain (Δ molar %/molar % ×100) calculated from (D) for DP 6 to DP 60 amylopectin chains of WT, *ss3a*, and *ss3a ss4b*. Values for the molar % in (D) for each DP represent the average of three seeds arbitrarily chosen from a single homozygous plant. The numbers on the plots represent the DP values.

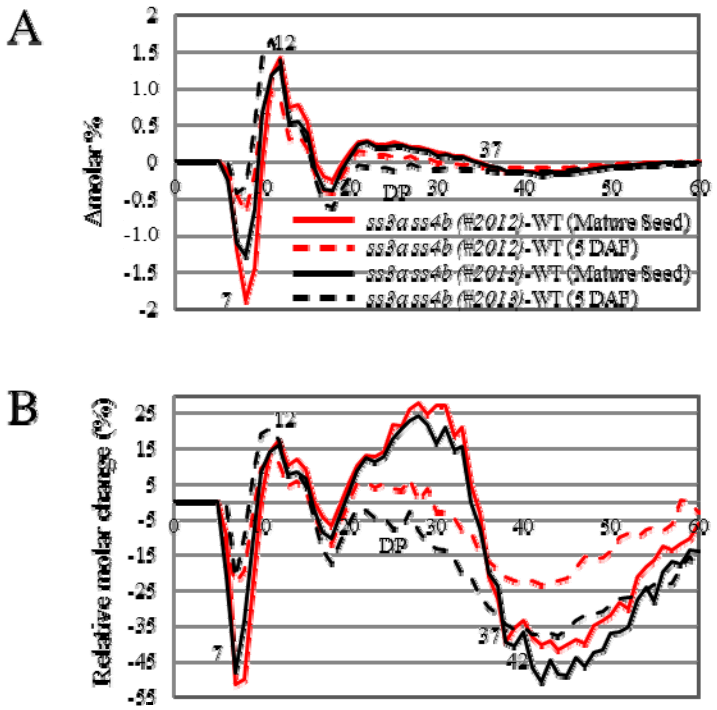

Supplemental Figure S7. Amylopectin chain-length distribution pattern in developing endosperm of mutant lines. A. Differences in chain-length distribution in developing endosperm at 5 DAF and mature endosperm of *ss3a ss4b* (*#2012*, *#2013*) and the wild-type (WT, Nipponbare).

B. Relative molar changes of each chain (Δ molar %/molar % × 100) calculated from (A) for DP 6 to DP 60 amylopectin chains of WT and *ss3a ss4b* (*#2012*, *#2013*). Values for molar % in (A) for each DP represent the average of three seeds arbitrarily chosen from a single homozygous plant. The numbers on the plots represent the DP values.

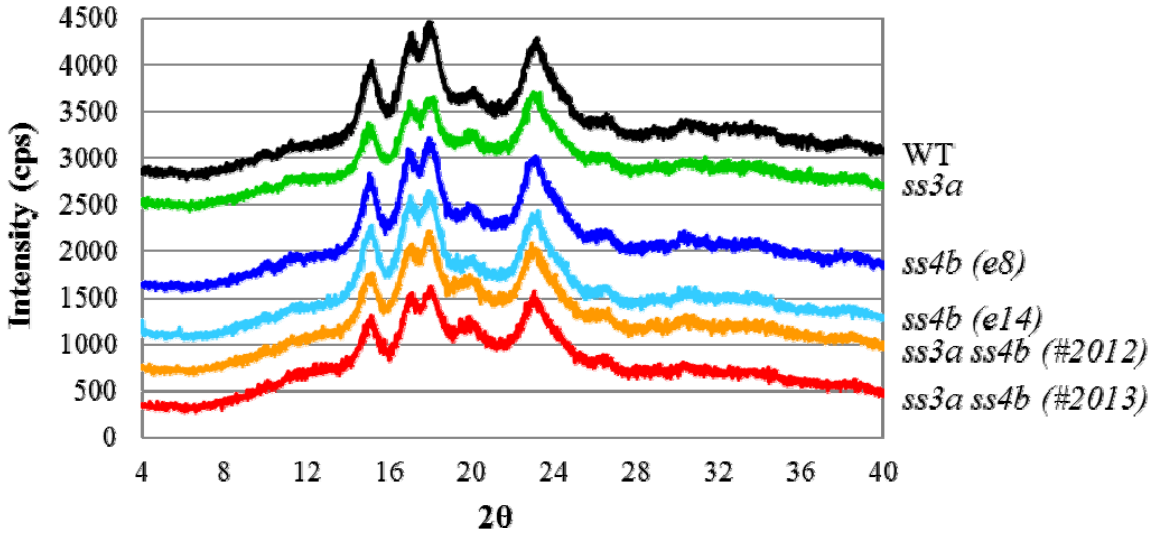

Supplemental Figure S8. X-ray diffraction patterns of endosperm starch in wild-type Nipponbare and mutant lines. WT, black line; *ss3a*, green line; *ss4b* (*e8*), blue line; *ss4b* (*e14*), light blue line; *ss3a ss4b* (#2012), orange line; and *ss3a ss4b* (#2013), red line.

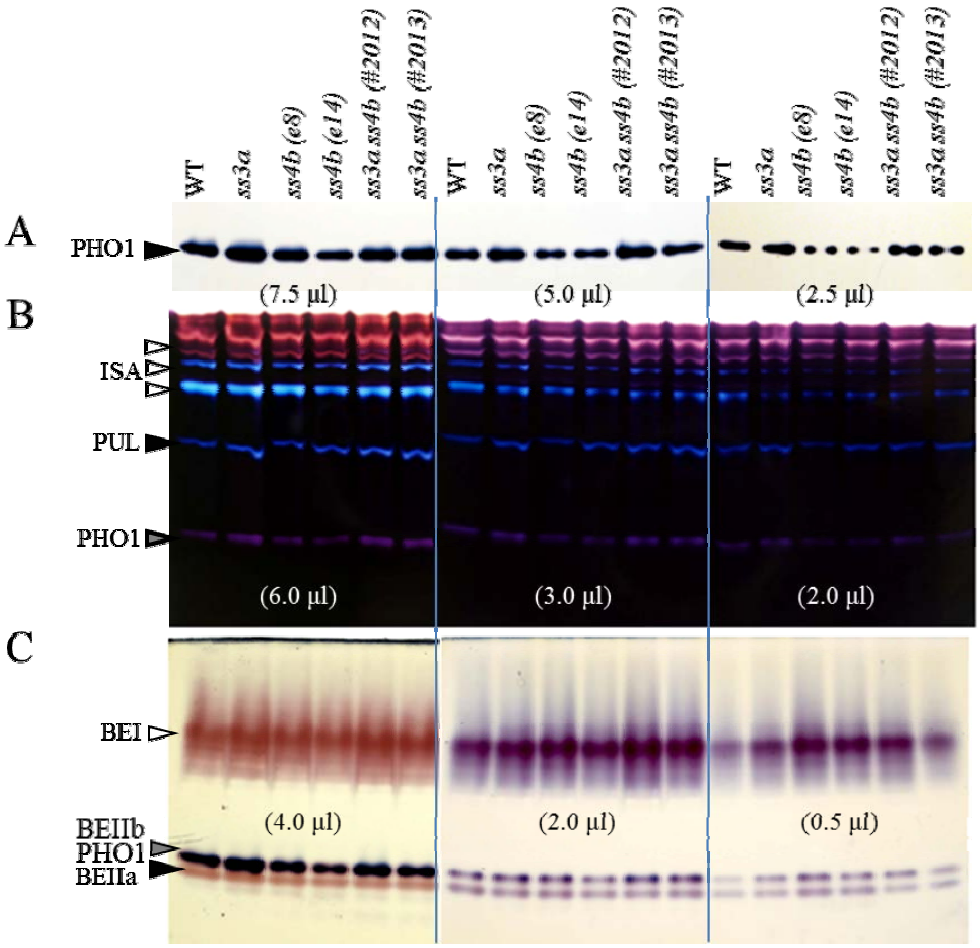

Supplemental Figure S9. Native PAGE staining for starch biosynthesis enzyme activity in the developing endosperm of the wild-type Nipponbare and mutant lines. A. Staining for PHO activity. Arrowhead indicates the PHO1 activity band. B. Staining for DBE activity. Arrowheads indicate the ISA, PUL, and PHO1 activity bands. C. Staining for BE activity. Arrowheads indicate the BEI, BEIIa, BEIIb, and PHO1 activity bands (the BEIIb and PHO1 bands overlap). The numbers in parentheses represent the volume of crude enzyme extract per lane.

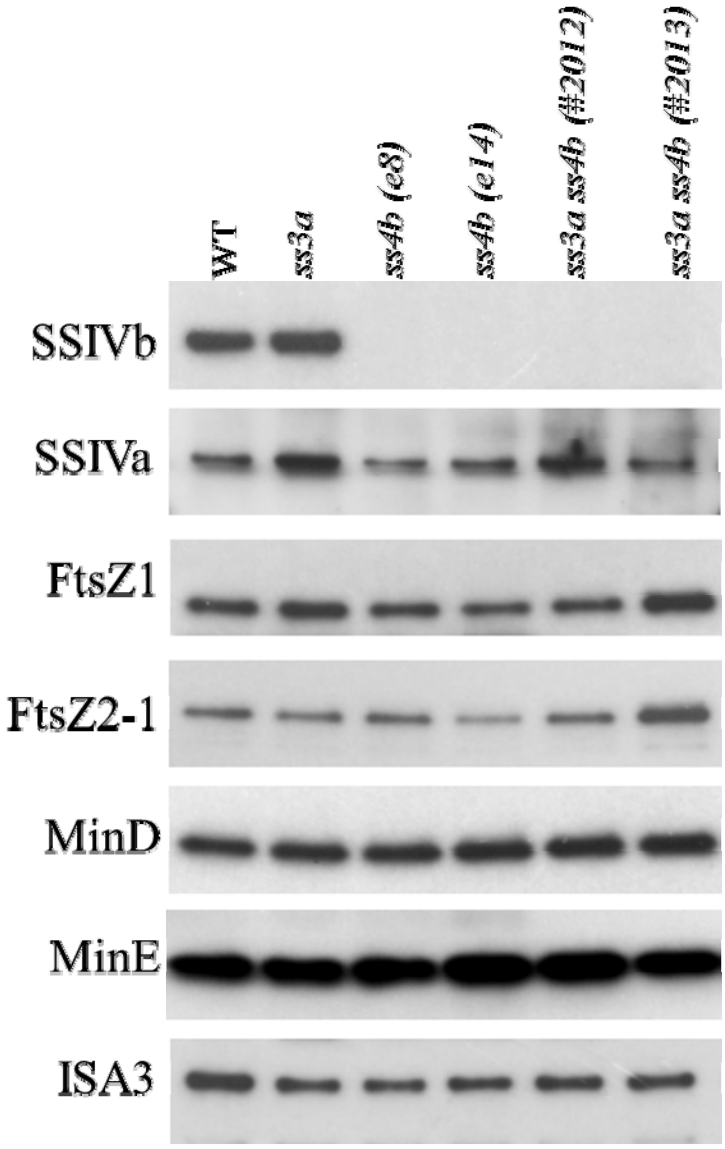

Supplemental Figure S10. Immunoblotting analyses with antibodies against SSIVb, SSIVa, FtsZ1, FtsZ2-1, MinD, MinE, and ISA3. Total protein was extracted from developing endosperm (7 DAF) of wild-type Nipponbare (WT) and mutant lines.

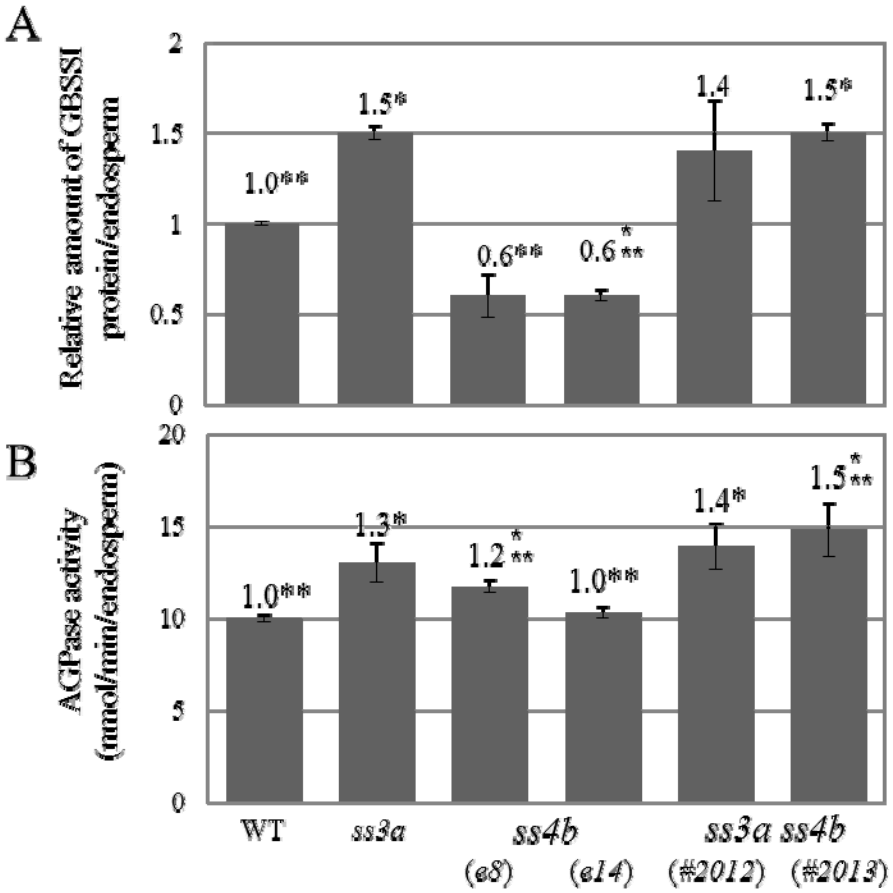

Supplemental Figure S11. Pleiotropic effects of SSIIIa and SSIVb deficiencies on GBSSI protein levels and AGPase activity. A, Amounts of GBSSI protein in mature endosperm of wild-type Nipponbare (WT) and mutant lines. B, AGPase activity in crude extracts of developing endosperm. Data are means ± SE of three seeds. Numbers on the graphs are relative to WT values. *Significant differences between WT and mutant lines (*t*-test, $P < 0.05$). **Significant differences between *ss3a* and other lines (*t*-test, $P < 0.05$).

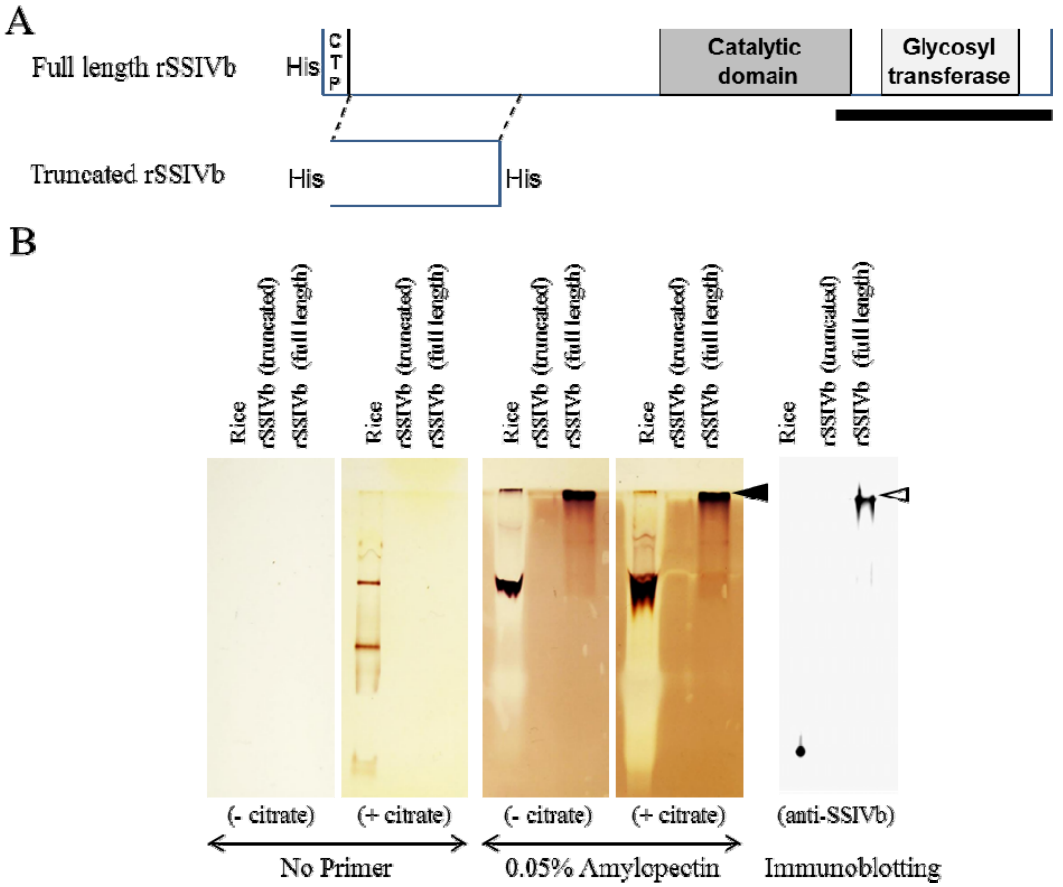

Supplemental Figure S12. Recombinant SSIVb (rSSIVb) exhibts SS activity. A, Scheme of the full-length and truncated SSIVb constructs for expression in *E. coli*. Truncated SSIVb lacks catalytic and glycosyltransferase domains. The underlined region was used as an antigen to generate SSIVb antibody. CTP, chloroplast transit peptide; His, 6 × histidine tag. B, Native PAGE, SS activity staining, and immunoblot of recombinant SSIVb. Native PAGE gels were prepared by addition of the indicated primers. Soluble proteins from wild-type Nipponbare and eluates from nickel chromatography of full-length or truncated rSSIVb were loaded. Gels were incubated with or without citrate in the reaction solution. The amylopectin-containing gel also was used for immunoblot with anti-SSIVb. Black arrowhead, rSSIVb activity band; white arrowhead, rSSIVb migrating at a similar position to the activity band.

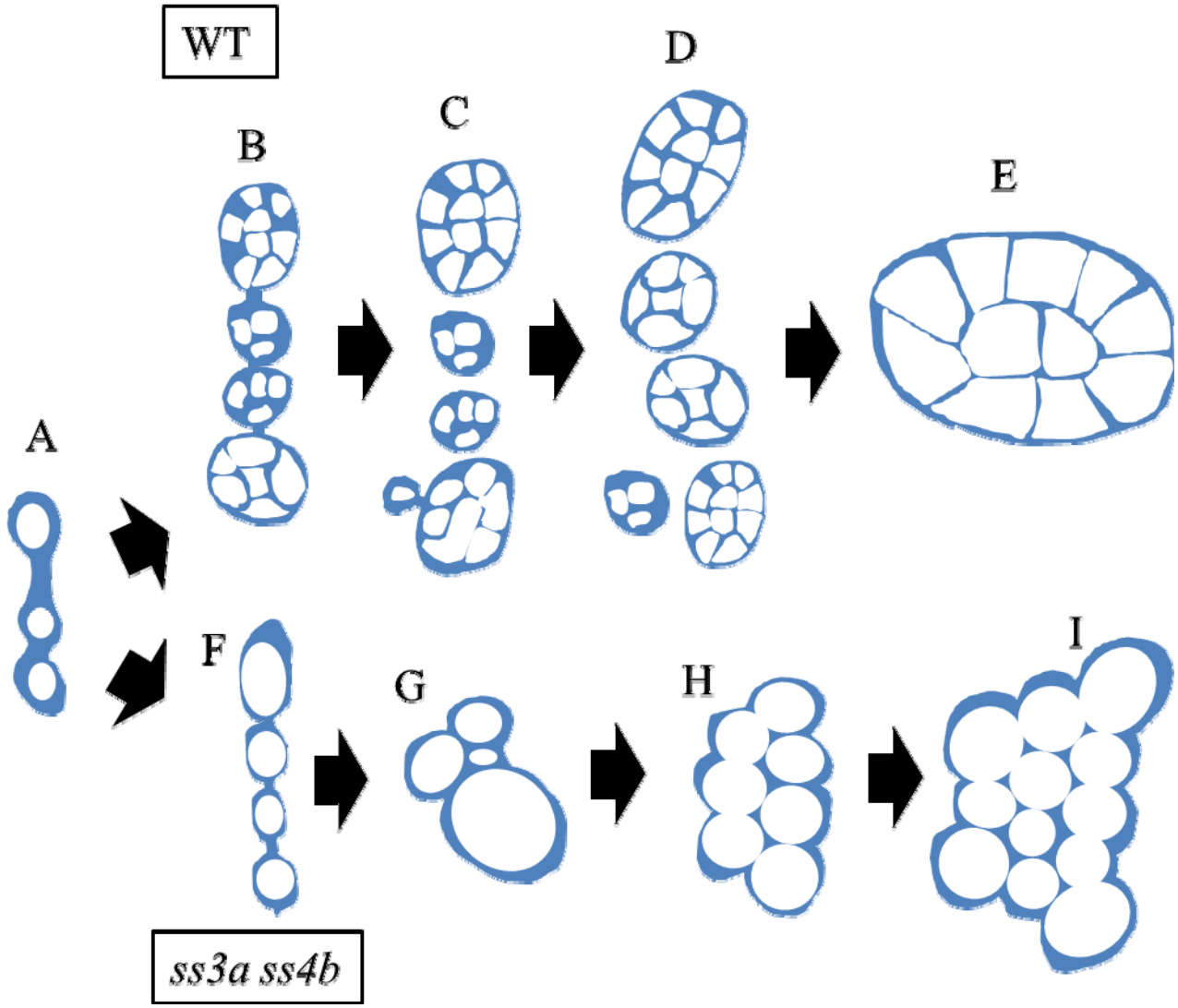

Supplemental Figure S13. Possible model of amyloplast development in early endosperm cells of wild-type (WT) and double mutant (*ss3a ss4b*). A–E and A–I indicate amyloplast development in WT and *ss3a ss4b*, respectively.